Tectonophysics 510 (2011) 337–344

Contents lists available at SciVerse ScienceDirect

Tectonophysics

journal homepage: www.elsevier.com/locate/tecto

Probing magnetic bottom and crustal temperature variations along the Red Sea margin of Egypt

D. Ravat [a,*], Ahmed Salem [b,c,d], A.M.S. Abdelaziz [d], E. Elawadi [d,e], P. Morgan [f]

[a] Dept. of Earth & Environmental Sciences, University of Kentucky, Lexington, KY 40506-0053, USA
[b] GETECH, Kitson House, Elmete Hall, Elmete Lane, Leeds, LS8 2LJ, UK
[c] School of Earth and Environment, University of Leeds, Leeds, LS2 9JT, UK
[d] Airborne Geophysics Dept, Exploration Division, Nuclear Materials Authority, P.O. Box 530 Maadi, Cairo, Egypt
[e] King Saud University, Saudi Arabia
[f] Colorado Geological Survey, 1313 Sherman Street, Room 715, Denver, CO 80203, USA

ARTICLE INFO

Article history:
Received 22 January 2011
Received in revised form 27 July 2011
Accepted 5 August 2011
Available online 16 August 2011

Keywords:
Eastern Egypt
Red Sea
Curie depth
Magnetic bottom
Heat flow
Magmatism

ABSTRACT

Over 50 magnetic bottom depths derived from spectra of magnetic anomalies in Eastern Egypt along the Red Sea margin show variable magnetic bottoms ranging from 10 to 34 km. The deep magnetic bottoms correspond more closely to the Moho depth in the region, and not the depth of 580 °C, which lies significantly deeper on the steady state geotherms. These results support the idea of Wasilewski and coworkers that the Moho is a magnetic boundary in continental regions. Reduced-to-pole magnetic highs correspond to areas of Younger Granites that were emplaced toward the end of the Precambrian. Other crystalline Precambrian units formed earlier during the closure of ocean basins are not strongly magnetic. In the north, magnetic bottoms are shallow (10–15 km) in regions with a high proportion of these Younger Granites. In the south, the shoaling of the magnetic bottom associated with the Younger Granites appears to be restricted to the Aswan and Ras Banas regions. Complexity in the variation of magnetic bottom depths may arise due to a combination of factors: i) regions of Younger (Precambrian) Granites with high magnetite content in the upper crust, leaving behind low Curie temperature titanomagnetite components in the middle and lower crust, ii) rise in the depth of 580 °C isotherm where the crust may have been heated due to initiation of intense magmatism at the time of the Red Sea rifting (~20 Ma), and iii) the contrast of the above two factors with respect to the neighboring regions where the Moho and/or Curie temperature truncates lithospheric ferromagnetism. Estimates of fractal and centroid magnetic bottoms in the oceanic regions of the Red Sea are significantly below the Moho in places suggesting that oceanic uppermost mantle may be serpentinized to the depth of 15–30 km in those regions.

© 2011 Elsevier B.V. All rights reserved.

1. Introduction

Despite our ability to compute temperatures through the solutions of the heat flow equation subject to boundary conditions (Carslaw and Jaeger, 1959), understanding lithospheric thermal structure and its local variation requires temperature constraints from all levels in the lithosphere. These constraints may take forms ranging from heat production and thermal conductivity at different levels, knowledge of seismic velocities at different depths, thickness of the crust and the lithosphere, estimates of basal heat flow into the lithosphere, and petrologic temperature constraints obtained from mantle xenoliths. In young tectonic regimes, when thermal steady state has not been achieved, constraints on timing, advection of heat, and basal heat flow may be needed to determine lithospheric temperatures. Many of these constraints are often not available.

Magnetic methods can help constrain the temperature in the crust through the phenomenon of Curie temperature (Tc). Above the Curie temperature (e.g., magnetite, Tc = 580 °C), magnetic minerals lose their ability of spontaneous magnetization and make deeper layers at greater temperatures essentially non-magnetic. This interface can be detected through a number of spectral magnetic methods (e.g., Bhattacharyya and Leu, 1975; Bouligand et al., 2009; Fedi et al., 1997; Maus et al., 1997; Okubo et al., 1985; Ravat et al., 2007; Ross et al., 2006; Spector and Grant, 1970; Tanaka et al., 1999).

While a magnetic constraint on the depth of the Curie temperature can be useful in steady state scenarios, the constraint is enormously important in modeling and understanding lithospheric temperatures in the situations when the basal and/or intrusion heat is in a transient phase and especially when that heat has not reached the surface and is not yet manifest in measurements of surface heat flow. The implications of this situation could be important for geothermal energy in some cases

* Corresponding author. Tel.: +1 765 720 0683; fax: +1 859 323 1938.
E-mail addresses: dhananjay.ravat@uky.edu (D. Ravat), paul.morgan@state.co.us (P. Morgan).

0040-1951/$ – see front matter © 2011 Elsevier B.V. All rights reserved.
doi:10.1016/j.tecto.2011.08.002

and also in understanding the behavior of rocks subject to stress (e.g., Afonso and Ranalli, 2004). Salem et al. (2000) studied the aeromagnetic data using spectral analysis and 2-D modeling techniques in parts of eastern Egypt. Their estimate of the Curie isotherm was as shallow as 10 km in the Quseir area (northern Red Sea margin), which they interpreted as heat flow greater than the average heat flow of the Red Sea margin and suggested that the area may be attractive for further geothermal exploration.

In this paper, we study the Red Sea margin of Egypt with the view toward understanding its crustal thermal structure through the concept of magnetic Curie depths. Morgan et al. (1985) and Boulous (1990) summarized the heat flow and other parameters in Egypt and suggested that, despite large local variation of along the Red Sea margin, heat flow appears to be decreasing with increasing distance inland from the coast. This understanding is consistent with the tectonic evolution of a young rifted margin with a zone of asthenospheric upwelling in the middle of the Red Sea as inferred from geologic, seismic refraction and gravity data in the northern Red Sea rift (Makris and Rihm, 1991).

2. Geologic background

Fig. 1 shows a schematic geologic map of eastern Egypt based on detailed maps of Egyptian Geological Survey and Mining Authority (1981) and Klitzsch et al. (1987). Lithologies of magnetic interest are exposed in the area of Precambrian basement along the eastern seaboard and constitute granites, metavolcanic units, and gneisses and migmatites. Granitoids and gneisses of the Precambrian of the Eastern Desert of Egypt formed during the Pan-African collisional and magmatic events that sutured different terranes (900–600 Ma) (Gass, 1977, 1981; Greiling et al., 1994; Hassan and Hashad, 1990). Of these units, Younger Granites or Calc-alkaline Granites (areas of higher proportion of these granites are demarcated as Zones A to E in Fig. 1), formed during 620–530 Ma subduction, amalgamation, and crustal remelting events, are strongly correlated with magnetic highs (Fig. 2), where they are exposed and mapped. The proportion of the exposed Younger Granites to other Precambrian units is high in the north, in latitudes between 25°N and 29°N (Zones A and B in Fig. 1), and in the south, from 22.5°N to 24°N (e.g., near Aswan at ~24°N, ~33°E; Hassan and Hashad, 1990). The correlation between the Younger Granites and the magnetic highs in the northern exposed Precambrian zone may make it possible to infer the batholithic expanses of these Younger Granites elsewhere underneath other older Precambrian units as well as younger overlying sedimentary formations surrounding the exposed Precambrian rocks. Based on the magnetic signature, the largest of these unexposed granitic batholithic masses may be on the west of the exposed Precambrian and in the area of Aswan.

Many models have been proposed for the evolution of the Red Sea ranging from purely active to purely passive rifting; none of them appears to be fully compatible with all of the evidence along the entire length of Red Sea, such as the timing of volcanism, uplift, and

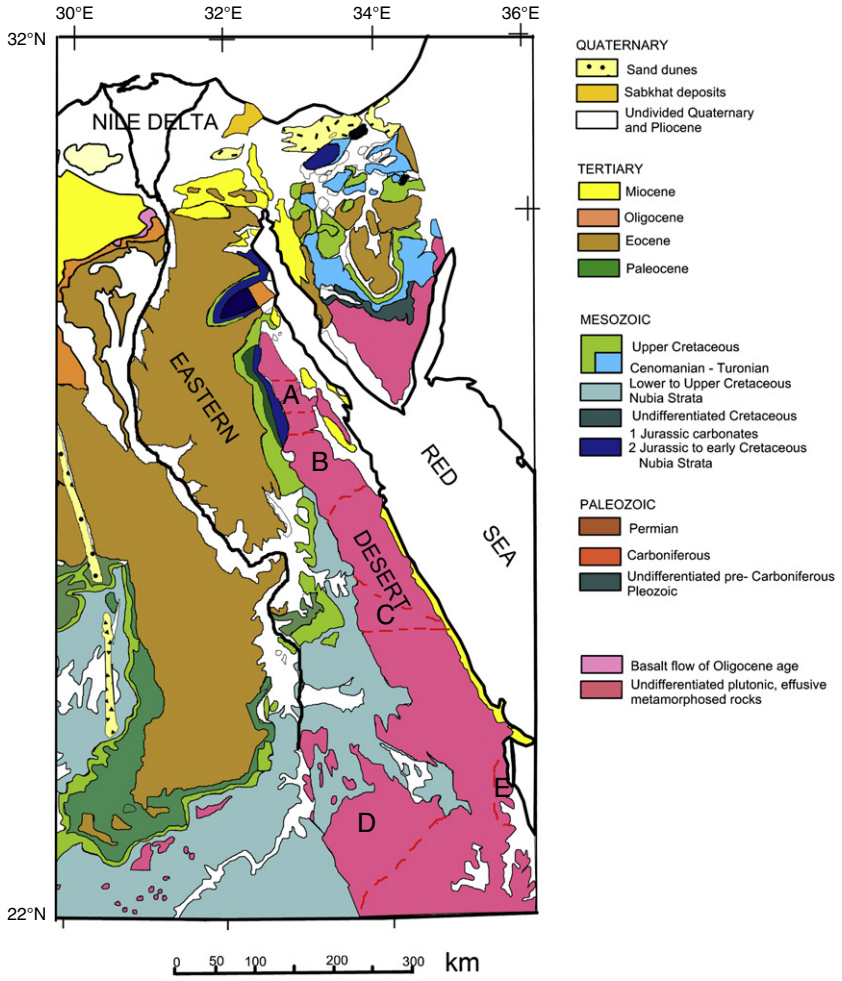

Fig. 1. Schematic of the eastern portion of the Geologic Map of Egypt based on the maps from the Egyptian Geological Survey and Mining Authority (1981) and Klitzsch et al. (1987) focusing primarily on the Precambrian crystalline rocks important for the magnetic interpretation in this study. Zones with higher concentrations of Calc-alkaline or Younger Granites within the Precambrian basement are enclosed in dashed lines and labeled A to E.

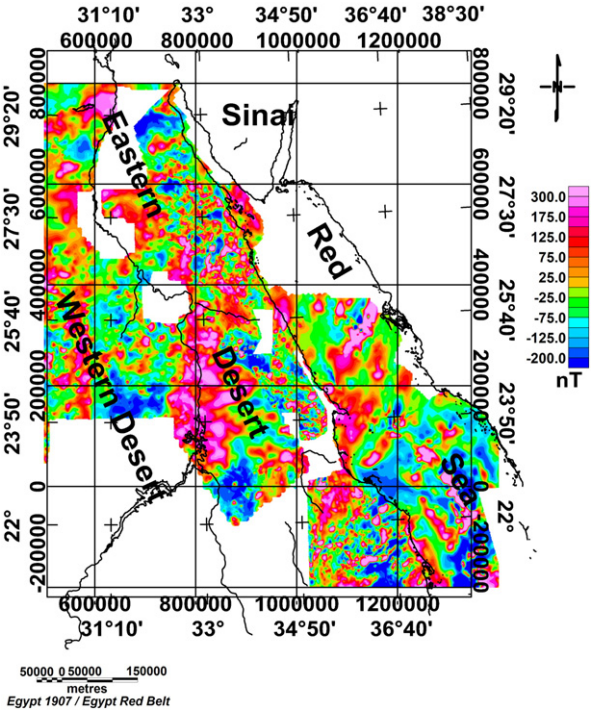

Fig. 2. The reduced-to-pole (RTP) magnetic anomaly map of the eastern portion of Egypt and part of the Red Sea. Many of the magnetic highs on this map are associated with the Precambrian Younger Granites (Zones A to E in Fig. 1).

extension (Ghebreab, 1998). In the northern Red Sea, magmatism intensified in the Miocene (~20 Ma, Izzeldin, 1987; Makris and Rihm, 1991). The Dead Sea strike slip faulting began at ~14 Ma which may be associated with the cause of seafloor formation of the northern Red Sea adjacent to Egypt (Makris and Rihm, 1991).

3. The magnetic bottom depth model studies

In referring to magnetic bottom depths derived through the interpretation of magnetic anomaly spectra, we use the term 'magnetic bottom' rather than the commonly used term 'Curie isotherm'; this is primarily because the continental Moho or other crustal layers can represent the bottom of magnetic layering for petrological reasons (e.g., Wasilewski et al., 1979) and the magnetic bottom is not always synonymous with the phenomenon of the Curie temperature. Three methods for estimating magnetic bottom from magnetic anomaly spectra used in the study are: i) centroid-based methods (34 estimates retained in the final analysis, Bhattacharyya and Leu, 1975; Okubo et al., 1985); ii) the method of forward modeling of the spectral peak (5 estimates where peaks were observed, Ross et al., 2006; Ravat et al., 2007); and iii) methods using fractal model magnetization (12 estimates, Maus et al., 1997; Bouligand et al., 2009). For the centroid-based and the spectral peak methods, we rely upon the model studies of Ravat et al. (2007). For the fractal method, we use the analytical expression of Bouligand et al. (2009) in which power spectra can be modeled from three parameters (Zt — depth to the top, Zthick — thickness of the layer, and β — the fractal parameter; Fig. 3).

Through our model studies, we found automatic non-linear parameter estimation method used by Bouligand et al. (2009) less reliable for this problem because the shape of the misfit residual is open-ended toward greater thicknesses and there are a number of reasonable solutions that lead to similar residual values and fit to the observed spectra as does the fit to the spectra having the minimum residual. We therefore prefer the complete parameter search approach and visual selection of alternative solutions in addition to the minimum L2-norm solution. We also found that the selection of the wavenumber range to be used from the spectra in the process of fitting the azimuthally-averaged wavenumbers was important. Sometimes the amplitudes of high wavenumbers do not monotonously decrease suggesting the presence of either variability in near-surface geologic sources or the presence of short-wavelength noise in the data; such wavenumbers should not be considered in fit of the modeled spectra.

To determine the existence of noise-prone high wavenumbers, we found that standard deviation proved to be a better error estimator than the two standard deviations of the standard error proposed by Bouligand et al. (2009). Standard error is an estimate of data error resulting from multiple observations of the same phenomenon; its error estimates decrease as $1/\sqrt{N}$, where N is the number of samples. Samples in the high wavenumber part of the azimuthally-averaged spectra come from different spatial locations and therefore should have large variance; however, because N is large for the high wavenumber region of azimuthally-averaged spectra, the standard error estimates turn out to be too small to reflect the realistic error in this part of the spectra. As a result of the issues related to selecting, modeling, and matching spectra, we did not find the approach of automatically determining the solution desirable. We decided to select first the wavenumber range to be fit (sometimes by trial and refinement) and then visually inspect all the solutions that fit the selected part of the spectra. After selecting the wavenumber range of the spectra to be fit, we did not consider error bars on the observations (such a consideration would lead to a large number of parameters) and instead we required that the model spectra fit the observed spectra visually as well as possible. Our model studies (see Fig. 3 and its caption, and Table 1) suggest that this approach generally led to usable if not perfect solutions. Based on our model studies, we found that the true solutions generally lie between the minimum residual norm and the knee of the minimum residual norm curve (see below).

Rarely can the minimum residual norm solution be successfully and correctly derived for all three parameters of the fractal method (Zt — depth to the top, Zthick — thickness of the layer, and β — the fractal parameter). The estimates improve significantly if one is able to a priori estimate either Zt or β; the estimates of Zt and β are also dependent on one another as shown by Bouligand et al. (2009). Bouligand et al. (2009) chose to fix β (to ~3 as it is the most often observed fractal parameter from various studies); however, we realized that it is much easier to estimate and fix the depth to the top of a magnetic layer (either from the fractal model fit to the high wavenumber part of the spectra, or the approaches suggested by Spector and Grant, 1970 and Fedi et al., 1997), or from the host of other available magnetic source depth determination techniques (e.g., The Euler method, Thompson, 1982; The Werner deconvolution, Werner, 1953; Hartman et al., 1971; Jain, 1976; The Tilt-depth method, Salem et al., 2010, etc.). In our model study, we also used different Zt and Zthick values to understand the performance of the method. Generally, the solution uncertainty is larger for thicker and/or deeper magnetic layers (see, for example, Table 1).

4. Mapping the magnetic bottom in the Eastern Desert along the Red Sea margin

Fig. 4 shows the map of the magnetic bottom derived from centroid-based, spectral peak, and fractal methods, independently derived by three of the coauthors using different software. There is a good agreement between the independently derived estimates (i.e., the differences between estimates from different methods in the same region were less than 5 km, which is roughly the uncertainty of individual spectral methods for deep crustal magnetic bottom depths). Whereas the surface heat flow decreases away from the Red Sea (Morgan et al., 1985), the magnetic bottoms are not a function of the

distance to the Red Sea rift. There appear to be alternating zones of deep (>20 km) and shallower (10–15 km) values all along the margin. The areas of shallow magnetic bottom encompass the locations of both high and low surface heat flows, indicating that the heat flow may partly be governed by hydrological regime. To some degree, the alternating shallow magnetic bottom regions are correlated with the zones of Younger (Precambrian) Granites (Calc-alkaline Granites) suggesting that the origin of this pattern may be partly mineralogical. However, the complexity in the magnetic bottom may be caused by other factors such as advection of heat during the Cenozoic rifting in the northern Red Sea. To examine this possibility, we investigated the lithospheric temperatures from modeling the surface heat flow values.

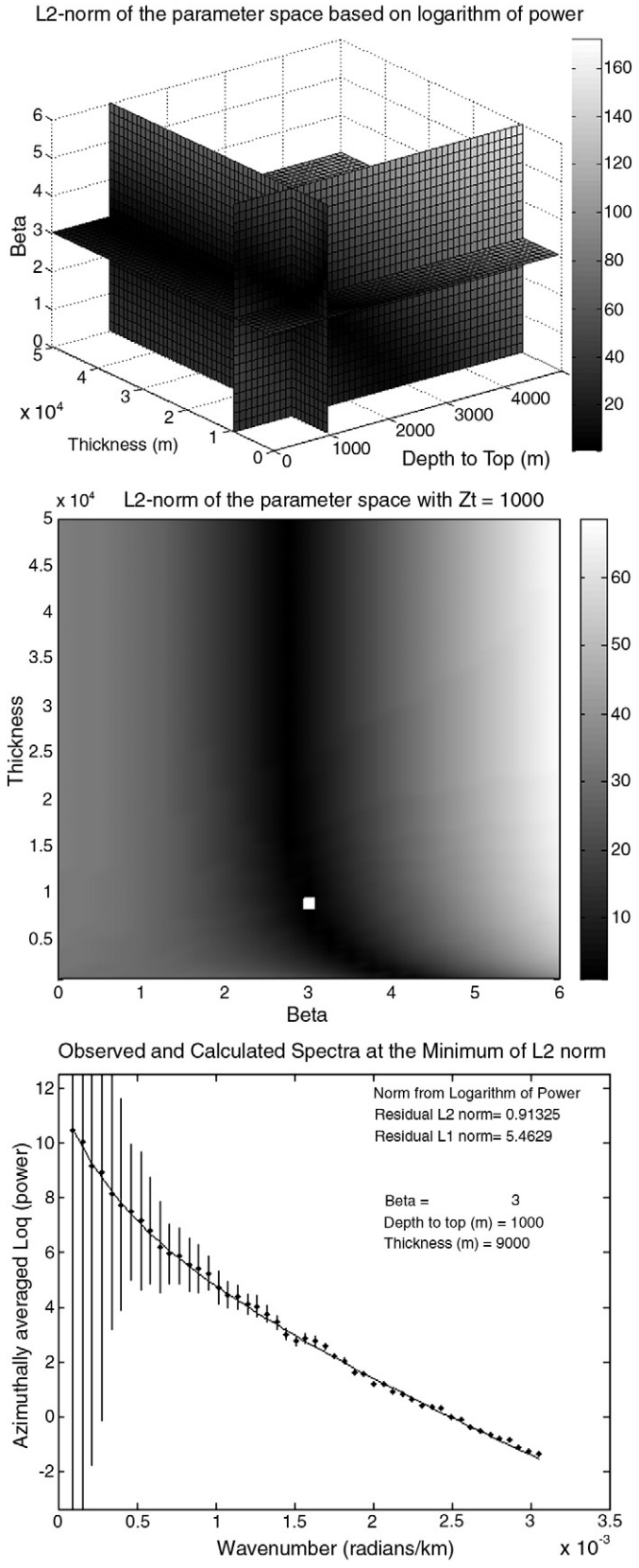

5. Steady state geotherms, the Moho, and the ferromagnetic bottom depth

Variability of surface heat flow observations is large (Boulous, 1990; Morgan et al., 1985) indicating the influence of hydrological circulation, and therefore, for initial thermal modeling, it is useful to use the conceptual model by Morgan et al. (1985) that suggests decrease in heat flow with the distance to the Red Sea margin. Fig. 5 shows a steady state geotherm model that reproduces the surface heat flow value at 200 km from the Red Sea margin using the approach of Lachenbruch and Sass (1978) and using the low end of the lithospheric thickness estimate of Pasyanos (2010) in the region (Table 2). Table 2 also lists the depths at which the geotherms intersect magnetite Curie temperatures, the maximum possible magnetic bottom depth at the given distance from this study, and the Moho depth/crustal thickness from Rihm et al. (1991) and Pasyanos and Nyblade (2007). In all three cases in Table 2, it appears that the maximum magnetic bottom in the Eastern Desert of Egypt is similar to the Moho depth rather than the steady state temperatures estimated from the modeling of the surface heat flow with lithospheric thickness constraints. It is also possible that lithospheric temperatures within 50–100 km inland from the Red Sea coast are in a transient state after rifting in the Red Sea region. Based on the abrupt nature of the continental margin in the region (Rihm et al., 1991), which suggests no reasons to anticipate significant rift-related magmatic activity affecting the continental interior, it seems reasonable that the lithosphere 200 km inland from the Red Sea coast may be in the steady state. Thus, the continental Moho here may indeed be the bulk ferromagnetic boundary. This is the one of the first pieces of direct magnetic anomaly based evidence that appears to support the hypothesis of the continental Moho as a magnetic boundary (Wasilewski et al., 1979; Wasilewski and Mayhew, 1992).

We also have a few estimates of the magnetic bottom from the Red Sea itself. In the northern Red Sea the Moho is observed around 10 km depth (Rihm et al., 1991) and at 11.5 and 18 km depth closer to the Sinai Peninsula (Mohamed and Miyashita, 2001). In the central and southern Red Sea (based on the model of Pasyanos and Nyblade, 2007) the Moho is estimated closer to 10 km depth. Some of the magnetic bottom depths agree closely with the Moho, but others are closer to 20 and 27 km depths (locations (1,275,000 m/50,000 m) and (1,050,000 m/300,000 m) in Fig. 4, respectively). It is possible that the sub-Moho uppermost mantle in some regions down to some 20–30 km depth is likely magnetic suggesting the existence of serpentinized peridotites under the Red Sea oceanic transition environment.

Fig. 3. Top) Mis-fit L2 norm over the parameter space of the fractal magnetic model with the depth to the top, Zt = 1000 m, magnetic layer thickness, Zthick = 10,000 m, and fractal parameter, β = 3. The minimum L2 norm mis-fit is at the intersection of three planes, Zt = 1000 m, Zthick = 9000 m, and β = 3. The parameter space was explored with the depth to the top ranging between 0 and 5000 m at 100 m spacing, thickness ranging between 1000 m to 50,000 m at 1000 m spacing, and β ranging between 0 and 6 at the interval of 0.25. The scale bar depicts the L2-norm residual for the parameter space. Middle) Mis-fit L2 norm over the parameter space of the same fractal magnetic model as above except that the solution with Zt constrained to 1000 m. White square shows the derived minimum L2 norm solution (Zthick = 9000 m and β = 3). The scale bar depicts the L2-norm residual for the parameter space. Bottom) Comparison of observed azimuthally averaged power spectrum (black symbols with vertical error bars of 1 standard deviation) and the best-fit power spectrum in the sense of residual L2 norm (continuous curve) for both the above runs.

Table 1
A model study with unconstrained three parameter and the depth to the top (Zt) constrained two parameter estimation. Zthick is layer thickness and β is fractal parameter. The comparisons shown here are examples of expected range of errors.

True Zt (m)	True Zthick (m)	True β	Unconstrained — 3 para: Zt (m)	Unconstrained — 3 para: Zthick (m)	Unconstrained — 3 para: β	Constrained at True Zt: Zthick (m)	Constrained at True Zt: β
1000	10000	3	1000	9000	3	9000	3
1000	5000	3	900	3000	3.25	6000	2.75
3000	10000	3	2600	6000	3.25	12000	2.5
3000	5000	3	2900	7000	2.75	9000	2.5
1000	20000	3	1000	24000	3	24000	3
1000	15000	3	900	11000	3.25	16000	3

There are many places within 50–100 km onshore of the coast where the magnetic bottoms are shallower than the Moho (Fig. 4). This indicates that there is a possibility that the surface heat flow is in a transient phase and the higher temperatures from the upwarped asthenosphere may have increased the temperatures in the middle crust within a zone roughly 100 km within the coast, but the heat may have only partly reached the surface. Forward modeling of the coastal surface heat flow values (~100 mW m^{-2}) with the lithospheric thickness of ~60 km (Pasyanos, 2010) suggests that strain rates of up to 1% must be included with the procedure of Lachenbruch and Sass (1978) in order to match the surface heat flow there. The additional heat flux due to stretching and intrusive activity is consistent with the rift scenario. Alternatively, the additional heat flow in rift situations can be reasoned using the thinning lithosphere model (Morgan, 1983).

6. The role of rift-stage intrusions in raising crustal temperatures

A regional gravity anomaly map of the region (Simple Bouguer on land and Free-air on ocean, Fig. 6) suggests that there lies a zone of dense (possibly mafic) intrusives along the eastern coast of Egypt. The map was constructed from CHAMP/GRACE 0.25° spacing Free-air gravity model (Eigen-GL05cp, Förste et al., 2007) and converted to Bouguer anomaly on land using the ETOPO5 elevation dataset and the topographic mass correction density of 2670 kg m^{-3}. The positive gravity anomalies range in width from roughly 20 km to 40–50 km and have amplitudes of 10–25 mGal. In the northern Red Sea, the rift appears to have bifurcated this zone of rift stage intrusions. Since there do not appear to be regional, exposed Tertiary intrusive rocks, it is likely that these intrusives lie deeper in the crust. Based on the width of the anomalies the intrusions may occupy a thicker zone of about 40 km opposite the southern portion of the Sinai Peninsula and also near the Ras Banas peninsula (24°N, 35.5°E).

Aeromagnetic maps over the intrusions on both the Egyptian side (Fig. 2) and the Saudi Arabian side are dominated by relatively short-wavelength features and the signature of the deeper intrusives is not apparent except where buried in the region west of the exposed Precambrian in the Eastern Desert and in the Aswan region (~24°N, ~33°E). The thick intrusive zone locations correspond to the zone of shallower magnetic bottom depths (10–15 km depth and within 50–75 km of the coast) and the shoaling may have been caused by the heat emitted by the intrusives. In this conceptual model, the intrusives may have heated the present middle crust, but the heat may not have reached the surface. Transient temperatures are feasible in this

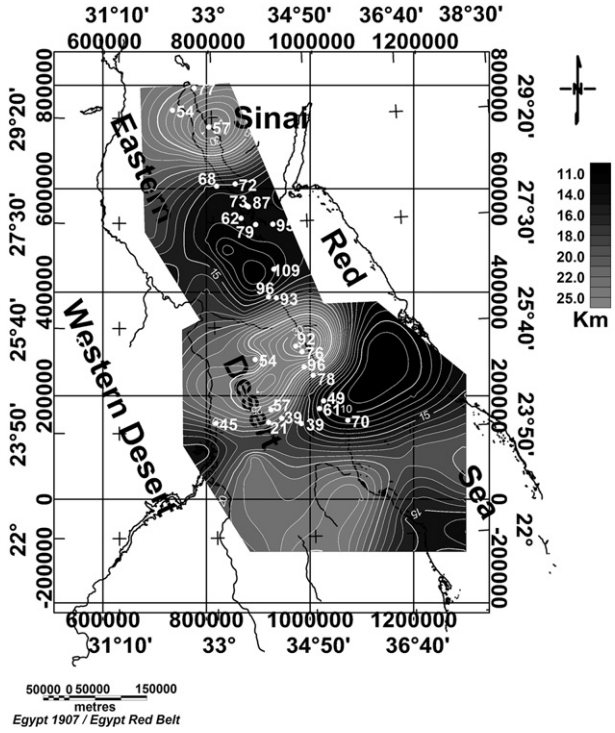

Fig. 4. Gridded depth to the magnetic bottom (gray shades and contours) from all magnetic bottom calculations used in this study. Bold numbers with filled circles are values surface heat flow (mW m^{-2}). Five alternating zones of deep/shallow magnetic bottoms can be identified. In the continental region, the areas of shallow magnetic bottom appear to be associated with the region of high proportion of exposed and interpreted Younger (Precambrian) Granites (see Fig. 1 and Geologic background).

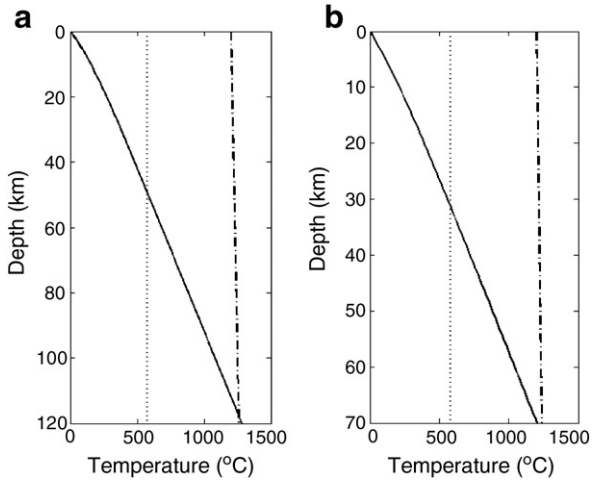

Fig. 5. Forward modeled geotherm from a steady state model of Lachenbruch and Sass with lithospheric thickness as a parameter. a) Geotherm at 200 km distance from the Red Sea coast matching the surface heat flow of ~45 mW m^{-2} from the conceptual model of Morgan et al. (1985). b) Geotherm at 50 km distance from the Red Sea coast matching the surface heat flow of ~60 mW m^{-2}. Lithospheric thickness ~120 km depth (part a) and ~70 km depth (part b) from surface wave tomography of Pasyanos (2010). For other parameters, see Table 2. The dash and dot lines are the adiabatic temperature gradient of 0.5 °C/km. The dotted lines on the figure are 580 °C (Curie temperature of magnetite); it intersects the geotherm at ~50 km (part a). The deepest magnetic bottom depth estimates are ~26–27 km and closely agree with the Moho depth suggesting that, in the continental regions of Egypt, magnetization terminates near the Moho at distances of 200 km from the Red Sea margin. Closer to the coast onshore, the Moho (~30 km) and the depth of the Curie temperature of magnetite are similar.

Table 2
Values of parameters used in the modeling of surface heat flow (from Morgan et al., 1985) using the derivation of Lachenbruch and Sass (1978). Thermal conductivity = 2.5 Wm^{-1} $°C^{-1}$; heat production = ~2.1 mW m^{-3} (Morgan et al., 1985); effective thickness of the heat production layer = 10 km. Lithospheric thickness estimates from Pasyanos (2010). Estimated crustal thickness from Rihm et al. (1991) and Pasyanos and Nyblade (2007). Adiabatic temperature gradient of 0.5 °C/km. The geotherms are shown in Fig. 5.

Distance from the Red Sea margin (km)	Mean observed and modeled (in [ ]) surface heat flow (mW m^{-2})	Lithospheric thickness (km)	Asthenospheric heat flow (mW m^{-2})	Depth (km) to 580 °C	Estimated crustal thickness (km)	Maximum magnetic bottom estimates (km)
50	60 [61]	70–80	40	~31	~26	~26
100	50 [51]	~100	30	~41	~28	~31–34
200	45 [46]	~120	25	~50	~25–32	~26–27

tectonic scenario given the timing of the initial rifting and they are necessary to explain the observed variation in the magnetic bottom depths.

We model this tabular zone of intrusions with the approximation that there could be 40 km width, long, dike-like intrusive zones at the coast reaching mid-crustal depths (rectangular parallelepiped model with an image source to maintain the surface temperature at 0 °C, Carslaw and Jaeger, 1959). The temperature increase for the case of a 40 km thick dike at 15 km depth is shown in Fig. 7(a). The intrusion temperatures are similar to molten mafic intrusives with the latent heat of solidification included (Carslaw and Jaeger, 1959). Based on the synthesis of Makris and Rihm (1991), the initial rifting and intensive magmatic activity occurred in the Miocene (~20 Ma). Because the crust/mantle surrounding the intrusion is likely to be at least at 400–600 °C, and because the temperature propagation will be controlled by the temperature differential, the intrusion is modeled with the temperature contrast of 700 °C. This model results in about 60°–80 °C present day temperature rise up to 20–30 km horizontally away from the intrusion at 20 Ma at mid-crustal depths. Adding the increased temperatures to the coastal steady state geotherm (Fig. 5b) does not raise the mid-crustal temperatures above the Curie temperature of magnetite (580 °C). If the mineralogy was titanomagnetitic with the Curie temperature of ~400°–450 °C, then such a mechanism would be feasible. The rise in the lower crustal temperatures in the neighborhood of the intrusion is about 100°–150 °C (graph not shown) and this is likely to make the present lower crust hotter than the Curie temperature of magnetite (also titanomagnetite) in the neighborhood of such intrusions. Since the Egyptian–Red Sea margin is abrupt (Makris and Rihm, 1991), one could assume a significantly wider intrusive zone (simulating the Red Sea width at 20 Ma); however, the temperature rise in the neighboring crust is neither significantly increased nor does it penetrate to distances farther inland.

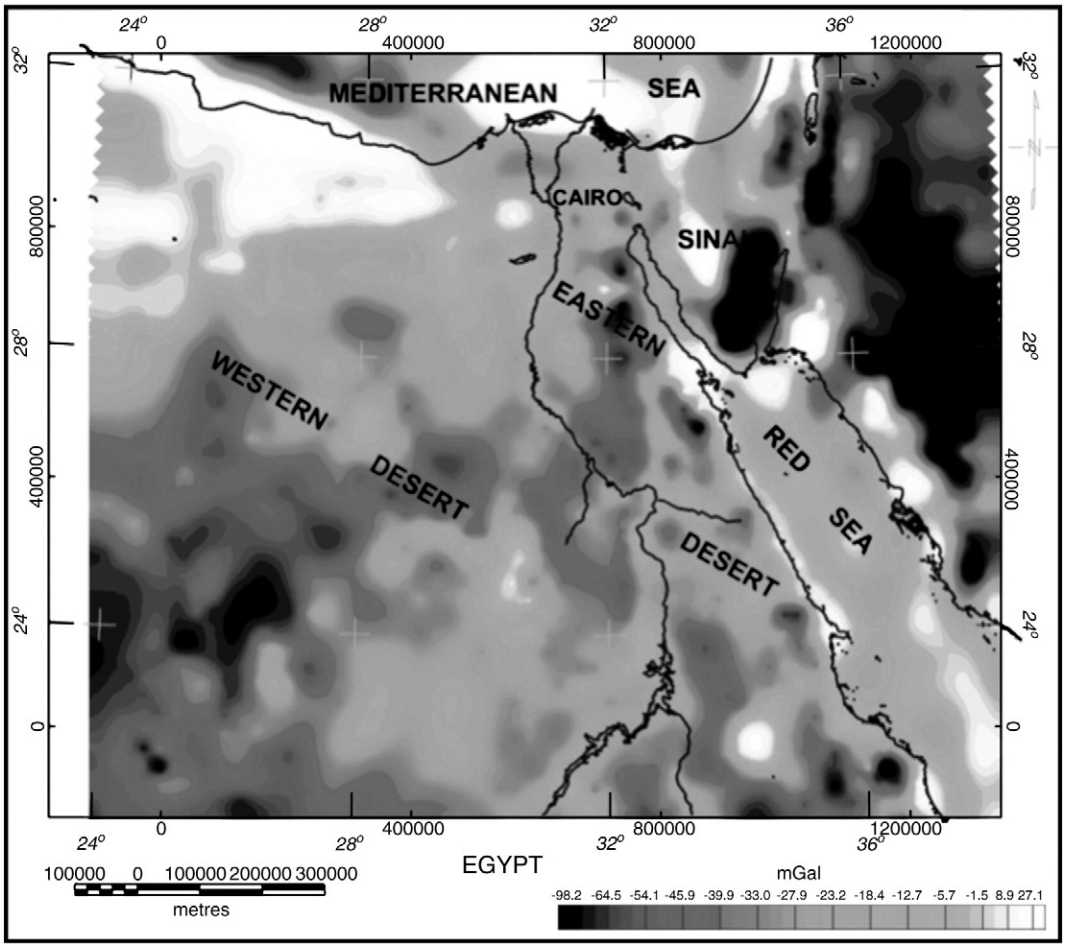

Fig. 6. A regional gravity anomaly map of Egypt and Red Sea at sea level based on joint CHAMP and GRACE satellite model Eigen-GL05cp and converted to Bouguer anomaly on land using ETOPO5 elevation model. Approximately 10–25 mGal highs (white color) of 20–40 km width straddle the coast of Egypt suggesting that mafic intrusives have been emplaced in this zone. The gravity highs across the Sinai and Ras Banas peninsula are wider suggesting the likelihood of more voluminous intrusive activity.

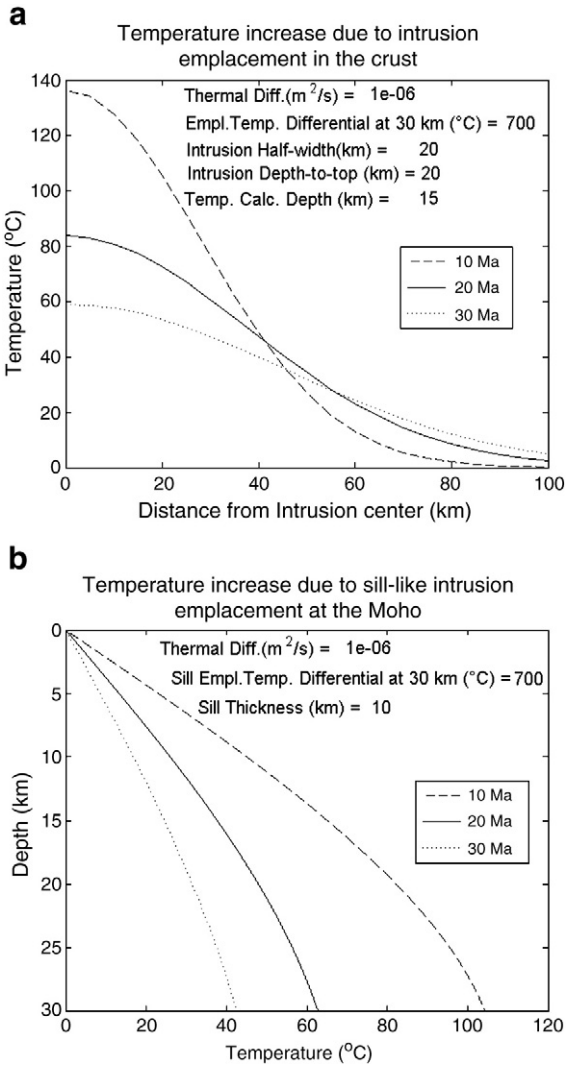

Fig. 7. (a) Temperature–distance–time relationships from a 40 km wide mafic intrusion deep in the crust on the Red Sea coast of Egypt. Initiation of rifting and intense intrusive activity took place in the Miocene (~20 Ma). The intrusion is able to raise temperatures by about 60°–80 °C some 20–30 km away from the intrusion. (b) Temperature–distance–time relationship above a 10 km thick sill at the Moho. The sill-like intrusion in the Miocene (~20 Ma) causes a temperature rise of about 50 °C in the middle crust.

Since dike-like intrusions cannot lead to a large temperature rise far away from them, we investigated temperature rise for a sill-like intrusion in the uppermost mantle (which may not be evident in gravity anomaly from lack of appreciable density contrast). For a 10 km sill-like intrusive source at the Moho depth, in the time span of 10–20 Ma, temperatures would rise by 40–70 °C in the middle crust (Fig. 7b) and examining the steady state geotherm at 50 km distance from the coast (Fig. 5b) that increase would also not be sufficient to drive the temperatures above the Curie point of magnetite in the middle crust; however, the rise is sufficient to do so in the lower crust. Considering the distances onshore from the coastline to which the magnetic bottoms have shallowed however (Fig. 4), combination of thick coastal intrusions, some interspersed intrusions into the Eastern Desert crust, some sill-like intrusive bodies in the uppermost mantle as well as titanomagnetitic mineralogy may be needed to account for the magnetic bottom depths observed in the region.

7. Discussion and conclusion

We have derived depths to magnetic bottom in the Eastern Desert of Egypt along the Red Sea margin. Over fifty magnetic bottom depths were derived from three different methods; the bottoms vary from 10 to 34 km. Results of the three methods are consistent with each other (i.e., locally they agree within a few km).

We find that the deepest of these depths (~26–27 km) at the distances of 200 km from the Red Sea margin are significantly shallower than the 580 °C isotherm depth (50–55 km depth) from modeling steady state geotherms which were constrained by the surface heat flow and the lithospheric thickness models. This depth corresponds more closely to the crustal thickness (~25–32 km) in the region and suggests that the Moho may be the magnetic bottom in this region, supporting the global postulate from rock magnetic analyses of mantle xenoliths by Wasilewski et al. (1979). However, closer to the coast, the temperatures near the Moho depth appear to be similar to the Curie temperatures of magnetite and hence one cannot distinguish between the two alternative mechanisms there.

Alternating zones of the derived east–west trending deep (>20 km) and shallow (10–15 km) magnetic bottom depths were mapped along the Red Sea margin of Egypt and their internal complexity cannot be explained by a single mechanism such as the heat from the Cenozoic (~20 Ma) rifting of the Red Sea or the crustal magnetic mineralogical variations. Reduced-to-pole magnetic anomaly highs correspond strongly with the locations of Younger (Precambrian) Granites (620–530 Ma). The regions of shallow magnetic bottom are closely allied with the locations of the Younger Granites, especially in the northern exposed Precambrian (26°N–28°N) and near Aswan (~24°N, ~33°E) where these granites are prolific. Away from the Cenozoic rift margin, the heat flow is also low and cannot lead to high temperatures in the middle crust. The radiogenic heat of the granites may not be significantly higher than in other Precambrian areas since, near Aswan, the heat flow is only 45 mW m^{-2}. Thus, at least away from the rifted margin, the cause of the shallow magnetic bottom may be in the magnetic mineralogy. Younger Granites magmatism resulted from remelting the middle and lower crust in the north during the process of cratonization (Hassan and Hashad, 1990) and as a consequence may have concentrated magnetite in the granitic plutons (in the upper crust and thus more correlated with magnetic anomaly highs), leaving middle and lower crust with titanomagnetite-bearing rocks with lower Curie temperatures (Haggerty, 1978), and thus are rendered non-magnetic.

In regions near the Cenozoic rift margin, the mid- and lower crustal temperatures may also be higher than the steady state due to the processes of rifting. Magmatism intensified in the northern Red Sea at ~20 Ma (Ghebreab, 1998; Izzeldin, 1987; Makris and Rihm, 1991) and the dissipation of heat from the cooling of the intrusives into the crust from that time could have warmed up the middle crust in the region close to the intrusions. Due to the timing of this activity, our illustrative calculations suggest that heat from the localized intrusions may have not reached the surface as it is not apparent in the surface heat flow data and the large part of surface heat flow variation near the coast may be hydrological.

Our estimates of fractal and centroid magnetic bottoms in the oceanic regions of the Red Sea are significantly deeper than the Moho (~10 km) suggesting that oceanic uppermost mantle may be serpentinized to the depth of 15–30 km in those locations.

Acknowledgments

We are grateful to the U.S.–Egypt Joint Board Scientific and Technological Cooperation and the U.S. National Science Foundation for funding this research under grant no. 0752764. We also thank Prof. Derek Fairhead and GETECH for making available some of the airborne magnetic anomaly data over Egypt used in this paper. We thank Prof. Randy Keller whose constructive review helped clarify parts of the manuscript. We also thank Prof. Mian Liu for his editorial work. Finally, D.R. thanks the Rockefeller Foundation's Bellagio Center for extending to him the spousal hospitality that made it possible to write the bulk of this paper.

References

Afonso, J.C., Ranalli, G., 2004. Crustal and mantle strengths in continental lithosphere: is the jelly sandwich model obsolete? Tectonophysics 394, 221–232.

Bhattacharyya, B.K., Leu, L., 1975. Analysis of magnetic anomalies over Yellowstone National Park. Mapping the Curie-point isotherm surface for geothermal reconnaissance. Journal of Geophysical Research 80 (32), 461–465.

Bouligand, C., Glen, J.M.G., Blakely, R.J., 2009. Mapping Curie temperature depth in the western United States with a fractal model for crustal magnetization. Journal of Geophysical Research 114, B11104.

Boulous, F.K., 1990. Some aspects of the geophysical regime of Egypt in relation to heat flow, groundwater and microearthquakes. In: Said, R. (Ed.), The Geology of Egypt. A.A. Balkema, Rotterdam/Brookfield, pp. 61–89.

Carslaw, H.S., Jaeger, J.C., 1959. Conduction of Heat in Solids. Oxford University Press, New York.

Egyptian Geological Survey and Mining Authority, 1981. Geologic Map of Egypt, 1, p. 2000000.

Fedi, M., Quarta, T., de Santis, A., 1997. Inherent power-law behavior of magnetic field power spectra from a Spector and Grant ensemble. Geophysics 62 (04), 1143–1150.

Förste, Ch., Flechtner, F., Schmidt, R., König, R., Meyer, U., Stubenvoll, R., Rothacher, M., Barthelmes, F., Neumayer, H., Biancale, R., Bruinsma, S., Lemoine, J.M., Loyer, S., 2007. Global mean gravity field models from combination of satellite mission and altimetry/gravimetry surface data. In: Fletcher, K. (Ed.), Proceedings of the 3rd international GOCE user workshop, ESA Publications Division, ESTEC, Noordwijk, The Netherlands, pp. 163–167, ISBN 92-9092-938-3, ISSN 1609-042X.

Gass, I.G., 1977. The evolution of the Pan African crystalline basement in NE Africa and Arabia. Journal of the Geological Society 134, 129–138.

Gass, I.G., 1981. Pan-African (upper Proterozoic) plate tectonics of the Arabian–Nubian Shield. In: Kroener, A. (Ed.), Precambrian Plate Tectonics. Elsevier, pp. 387–405.

Ghebreab, W., 1998. Tectonics of the Red Sea region reassessed. Earth-Science Reviews 45, 1–44.

Greiling, R.O., et al., 1994. A structural synthesis of the Proterozoic Arabian–Nubian Shield in Egypt. Geologische Rundschau 83, 484–501.

Haggerty, S.E., 1978. Mineralogical constraints on Curie isotherms in deep crustal magnetic anomalies. Geophysical Research Letters 5 (2), 105–108.

Hartman, R.R., Tesky, D.J., Friedberg, J.L., 1971. A system for rapid digital aeromagnetic interpretation. Geophysics 36, 891–918.

Hassan, M.A., Hashad, A.H., 1990. Precambrian of Egypt. In: Said, R. (Ed.), The Geology of Egypt. A. A. Balkema, Rotterdam, pp. 201–248.

Izzeldin, A.Y., 1987. Seismic, gravity and magnetic surveys in the central part of the Red Sea: their interpretation and implications for the structure and evolution of the Red Sea. Tectonophysics 143, 269–306.

Jain, S., 1976. An automatic method of direct interpretation of magnetic profiles. Geophysics 41, 531–541.

Klitzsch, E., List, F.K., Pöhlmann, G., 1987. Geological Map of Egypt. Conoco. 1:500,000, 20 sheets.

Lachenbruch, A.H., Sass, J.H., 1978. Models of an Extending Lithosphere and Heat Flow in the Basin and Range Province. Memoir Geological Society of America. pp. 209–250.

Makris, J., Rihm, R., 1991. Shear-controlled evolution of the Red Sea: pull apart model. Tectonophysics 198, 441–446.

Maus, S., Gordon, D., Fairhead, D., 1997. Curie-temperature depth estimation using a self-similar magnetization model. Geophysical Journal International 129 (1), 163–168.

Mohamed, H., Miyashita, K., 2001. One-dimensional P-wave velocity structure in the northern Red Sea area, deduced from travel time data. Earth Planets Space 53, 695–702.

Morgan, P., 1983. Constraints on rift thermal processes from heat flow and uplift. Tectonophysics 84, 277–298.

Morgan, P., et al., 1985. Heat flow in eastern Egypt: the thermal signature of a continental Breakup. Journal of Geodynamics 4, 107–131.

Okubo, Y., Graf, R.J., Hansen, R.O., Ogawa, K., Tsu, H., 1985. Curie-point depths of the island of Kyushu and surrounding areas, Japan. Geophysics 50 (3), 481–494.

Pasyanos, M.E., 2010. Lithospheric thickness modeled from long-period surface wave dispersion. Tectonophysics 481, 38–50.

Pasyanos, M.E., Nyblade, A.A., 2007. A top to bottom lithospheric study of Africa and Arabia. Tectonophysics 444, 27–44.

Ravat, D., Pignatelli, A., Nicolosi, I., Chiappini, M., 2007. A study of spectral methods of estimating the depth to the bottom of magnetic sources from near-surface magnetic anomaly data. Geophysical Journal International 169 (2), 421–434.

Rihm, R., Makris, J., Möller, L., 1991. Seismic surveys in the Northern Red Sea: asymmetric crustal structure. Tectonophysics 198, 279–295.

Ross, H.E., Blakely, R.J., Zoback, M.D. , 2006. Testing the use of aeromagnetic data for the determination of Curie depth in California. Geophysics 71, L51–L59.

Salem, A., Ushijima, K., Elsirafi, A., Mizunaga, H., 2000. Spectral analysis of aeromagnetic data for geothermal reconnaissance of Quseir area, northern Red Sea, Egypt. Proceedings of World Geothermal Congress. Kyushu-Tohoku, Japan, pp. 1669–1673.

Salem, A., Williams, S., Samson, E., Fairhead, D., Ravat, D., Blakely, R.J., 2010. Sedimentary basins reconnaissance using the magnetic Tilt-Depth method. Exploration Geophysics 41, 198–209.

Spector, A., Grant, F.S., 1970. Statistical models for interpreting aeromagnetic data. Geophysics 35, 293–302.

Tanaka, A., Okubo, Y., Matsubayashi, O., 1999. Curie point depth based on spectrum analysis of the magnetic anomaly data in East and Southeast Asia. Tectonophysics 306, 461–470.

Thompson, D.T., 1982. "EULDPH" — a new technique for making computer-assisted depth estimates from magnetic data. Geophysics 47, 31–37.

Wasilewski, P.J., Mayhew, M.A., 1992. The Moho as a magnetic boundary revisited. Geophysical Research Letters 19 (22), 2259–2262.

Wasilewski, P.J., Thomas, H.H., Mayhew, M.A., 1979. Moho as a magnetic boundary. Geophysical Research Letters 6 (7), 541–544.

Werner, S., 1953. Interpretation of Magnetic Anomalies at Sheet-like Bodies: Sverges Geologiska Undersok. Ser. C. c. Arsbok 43, N:06.